Supporting information

A cyclic brush zwitterionic polymer based pH-responsive nanocarrier-mediated dual drug delivery system with lubrication maintenance for osteoarthritis treatment

Miao Zhang,[a] Xu Peng,[b] Yuan Ding,[a] Xiang Ke,[a] Kai Ren,[a] Qiangwei Xin,[a] Meng Qin,[a] Jing Xie*[a] and Jianshu Li*[a,c,d]

[a] College of Polymer Science and Engineering, State Key Laboratory of Polymer Materials Engineering, Sichuan University, Chengdu 610065, P.R. China

[b] Experimental and Research Animal Institute, Sichuan University, Chengdu 610065, P.R. China

[c] State Key Laboratory of Oral Diseases, West China Hospital of Stomatology, Sichuan University, Chengdu 610041, P.R. China

[d] Med-X Center for Materials, Sichuan University, Chengdu 610041, P.R. China

* Corresponding author: Jing Xie, Jianshu Li

E-mail addresses: xiej@scu.edu.cn (J. Xie), jianshu_li@scu.edu.cn (J. Li).

List of contents

1. Experimental section

1.1 Materials.

Bipyridine (bpy, TCI, 98%), copper(I) bromide (CuBr, Macklin, 99%), Triethylamine (TEA, Macklin) and *N*, *N*, *N*′, *N*″, *N*″-pentamethyldiethylenetriamine (PMDETA, Macklin, 99%). 2-(Dimethylamino) ethyl methacrylate (DMAEMA, Aladdin, 99%) and 2-Hydroxyethyl methacrylate (HEMA, 99%, J&K) were purified by passing through a basic Al_2O_3 alumina column to remove the inhibitor. [2-(Methacryloyloxy)ethyl]dimethyl-(3-sulfopropyl) (SBMA, Aladdin, ≥97%). 2-bromoisobutyryl bromide (J&K). Sodium azide (NaN_3, Sanyou, Shanghai). Dichloromethane (DCM), isopropyl alcohol (IPA, 99.7%) and methyl alcohol (Bodi, Tianjin, china). *N*, *N*-dimethyl formamide (DMF, 99.5%) (Paini, Zhengzhou, china). Diethy ether anhydrous (Xilongkexue, Sichuan, china). 2,2,2-Trifluoroethyl alcohol (TFEA, 99.8%, Adamas-beta, Shanghai). Curcumin (Cur, ≥98%, Beijng Solarbio Science & Technology Co., Ltd.) and Loxoprofen sodium (LXP, Solarbio, ≥98%). T-AOC Assay Kit, Cell Counting Kit-8 (CCK-8) and Reactive Oxygen Species Assay Kit (ROS Assay Kit) were purchased from beyotime biotechnology. TRITC Phalloidin (300T, Solarbio). DAPI, PI staining solution and trizol reagent were purchased from Solarbio. PBS and all consumables for cell research were purchased from Baoxin Biotechnology Co., LT. Serum inflammation detection kit for SD rats were purchased from Jiangsu Meimian Industrial Co., Ltd. Rat chondrocytes and complete medium (DM/F 12, including FBS, EGF, insulin, trans ferrin, telenium solution, penicillin, streptomycin, etc.) were purchased from “Procell Life Science &

Technology Co., Ltd".). SD rats were provided Jiang'an Campus of Sichuan University (Chengdu, China). All other reagents were of analytical grade and used as received.

1.2 Instruments and measurements.

The chemical structures of the synthesized polymers were characterized by ^{1}H NMR spectra, which recorded on an AV III HD spectrometer at 400 MHz using $CDCl_3$, DMSO-d_6 and D_2O as the solvents. The FT-IR spectroscopic measurements were conducted on a NEXUS 670 FT-IR spectrometer (Nicolet, WI, USA). Samples were pressed into potassium bromide (KBr) pellets prior to the measurements. The molecular weight (MW) and polydispersity index ($Đ$) of all of the synthesized polymer samples were determined by size-exclusion chromatography and multi-angle laser light scattering (SEC-MALLS) and using HPLC-grade DMF containing 0.1 wt% LiBr at 60 °C as the eluent at a flow rate of 1 mL/min. The MALLS detector was operated at a laser wavelength of 690.0 nm. The polymer solution was prepared in phosphate buffer solution (PBS, pH 7.4, 150 mM) and saline sodium citrate (SSC, pH 5.5, 150 mM) at a concentration of 1 mg/mL.

The average hydrodynamic size of the micelles was measured by using dynamic light scattering (DLS) on a Zetasizer (Nano ZS, Malvern, Worcestershire, UK) at a fixed detection angle of 173^o at 25 °C. The transmission electron microscope (TEM) was operated on JEOL JEM-2100 at an accelerating voltage of 20-200 keV. Scanning electron microscopy (SEM): The microstructure of polymers was observed using SEM (ThermoFisherScientific FEI, Tokyo, Japan). Briefly, the polymer solution was

dropped onto a silicon wafer, coated with a thin layer of gold and then observed using accelerating voltage of 5 kV. Atomic force microscopy (AFM) measurements were taken on a Bruker Dimension ICON Atomic Force Microscope in tapping mode in air at 25 ℃ with OLTESPA-R3 silicon nitride tips. The samples were prepared by dropping an aqueous solution of 0.02 mg/mL onto a mica wafer.

1.3 Synthesis of *a*-functionalized initiators.

Propargyl 2-bromoisobutyrate was synthesized as described in the literature.[1]

1.4 Synthesis of linear precursor (*l*-P(HEMA)$_{50}$-N$_3$).

The *l*-P(HEMA)$_{50}$-Br and *l*-P(HEMA)$_{50}$-N$_3$ were synthesized by similar methods reported in literature.[2] Briefly, *l*-P(HEMA)$_{50}$-Br was prepared by ATRP of HEMA using propargyl 2-bromoisobutyrate as the initiator and bpy/CuBr as the catalysin with the molar ratio of monomer, initiator, catalyst and ligands (HEMA/Initiator/CuBr/bpy=50/1/1/2). Furthermore, the linear precursor with an azide terminus was obtained by the substitution reaction of *l*-P(HEMA)$_{50}$-Br and NaN$_3$.

1.5 Synthesis of cyclic polymer (*c*-P(HEMA)$_{50}$) and c-P(HEMA-Br)$_{50}$.

c-P(HEMA)$_{50}$ and *c*-P(HEMA-Br)$_{50}$ were synthesized as described in the previously literature.[3]

1.6 Preparation of self-assembled micelles.

Generally, 2 mg of copolymers was dissolved in 2 mL of deionized water and sonicated for 30 min to complete dissolution. Ultimately, micelle solution with a concentration of approximately 1.0 mg/mL was obtained.

Dynamic light scattering (DLS) was used to determine the average hydrodynamic

size of micelles on a Zeta sizer (Nano ZS, Malvern, Worcestershire, UK) with the detection angle fixed at 173°. Note that all data were gained from the average of three tests. The sample solution was passed through a Millipore 0.45 μm pore-sized syringe filter prior to measurements. Polymer solutions with concentrations of 1.0 mg/mL were evaluated.

Zeta potential was used to determine the stability of the dispersed system. The test was performed by injecting a sample of the measured concentration (1.0 mL-1.5 mL) into the sample pool, which was then inserted into the instrument and waited for temperature to equilibrate, and then perform the test. Note that all data were gained from the average of three tests.

The morphology of the polymer samples was observed by TEM on JEM-2100 at an accelerating voltage of 200 keV. To prepare specimens for TEM observation, a drop of micelle solution (1 mg/mL) was deposited onto a carbon-coated copper grid. After deposition, excess solution was removed using a strip of filter paper. The phosphotungstic acid (2 % w/w) was used as negative staining and stained the sample for 5 min. Finally, the sample was dried in air.

1.7 Lubrication property.

The lubrication property of BB and CBs aqueous solution were evaluated through tribological tests. Tribological tests were performed in reciprocating mode at room temperature on a multifunctional friction and wear tester (UMT-3, Bruker, USA). All the tribology experiments adopted the ball-disk friction test mode, and Si_3N_4 ball and polytetrafluorethylene (PTFE) were used as upper and lower friction pairs. Friction

tests were performed for 10 min at different lubricant concentrations (0.25-5.0 mg/mL), loads (1-3 N) and frequencies (0.5-3 Hz). Specifically, 1 mL lubricant sample was dropped on the contact area and deionized water (DI) was used as the control group. The sliding speed was set as 3 mm/s and the sliding amplitude was set as 3 mm. The curves of friction coefficient (COF) of each lubricant with time were recorded under different concentrations, loads and frequencies to evaluate the lubrication performance of each lubricant. After the friction test, the surface roughness of the samples was observed with confocal laser scanning microscope (Zeiss LSM799 MAT) to evaluate the wear performance.

1.8 Extracellular ROS scavenging activity.

The ROS scavenging activity of CB@Cur@LXP was determined by DPPH, H_2O_2 and total antioxidant capacity, respectively.

1.8.1 Scavenging of DPPH by CB@Cur@LXP.

The scavenging capability of different samples on DPPH radical was measured by the method reported in literature. Briefly, 4 mg DPPH was dissolved in 10 mL ethanol solution to obtain DPPH ethanol solution, which was then diluted to the target concentration (0.1 mM, 2 mL). DPPH ethanol solution (0.1 mM, 800 μL) was incubated with different samples (0.25 mg/mL, 800 μL) for 30 min in dark at 37 °C. Finally, the DPPH (100 μL) and polymer solution (100 μL) were added to the 96-well plate, and the absorbance at 517 nm was recorded by microplate reader. The DPPH radical elimination was calculated using the following equation:

$$\text{DPPH elimination (\%)}=(1-\frac{A_{sample517}}{A_{control517}})$$

where $A_{sample517}$ is the absorbance of the mixture with various sample, and $A_{control517}$ is the absorbance of control solution only containing DPPH without sample.

1.8.2 Scavenging of H_2O_2 by CB@Cur@LXP.

The H_2O_2 scavenging capacity of different polymers was measured by Hydrogen Peroxide Assay Kit. The specific operation is based on the instruction of the H_2O_2 content detection kit. Briefly, (1) preparation of solution: preparation of 1 nm H_2O_2 solution and dissolution of reagent 2 (HCl, 3 mL). (2) Samples of incubation: the experimental group (sample + H_2O_2) and the control group (sample + H_2O) were incubated at 37 ℃ for 4 h, respectively. (3) Sample preparation: 250 μL of each incubation sample was put into EP tubes, and 25 μL reagent 2 and 50 μL reagent 3 were added to each tube successively. At this time, flocculent appeared in the EP tube, and the supernatant was removed by centrifugation, and then 250 μL reagent 4 was added to dissolve the precipitate. Finally, 80 μL samples were added to the 96-well plate, and the absorbance of each well at 415 nm was recorded by microplate reader.

1.8.3 Evaluation of total antioxidant capacity at CB@Cur@LXP.

The total antioxidant capacity of different polymers was measured using the T-AOC Assay Kit.[4,5] Specifically, an appropriate amount of FRAP working solution was prepared based on the number of samples to be measured (including the standard curve), and the working solution was incubated for 1 h in dark at 37 °C. The preparation of FRAP working solution is as shown in the total antioxidant capacity detection kit (FRAP method) provided by beyotime biotechnology.

Determination of standard curves: 27.8 mg $FeSO_4 \cdot 7H_2O$ was dissolved in 1 mL deionized water (100 mM), and an appropriate amount of 100 mM $FeSO_4$ solution was diluted to 1.0 mM.

Determination of total antioxidant capacity: (1) Add 180 μL of FRAP solution to 96-well plate to be tested. (2) Add 5 μL distilled water into the blank control well; add 5 μL of $FeSO_4$ standard solution of various concentrations into the test well; add 5 μL of various samples or 1.0 mM Trolox into the sample test well as positive control, and gently shake the well plate. (3) The reaction mixture was shaken and incubated for 5 min at 37 °C, and the absorbance of the solution was recorded at 593 nm. (4) The total antioxidant capacity of the samples was calculated according to the standard curve.

1.9 *In vitro* drug loading and drug release study of pH-sensitive bottle brush and cyclic brush polymers.

The hydrophobic drug curcumin (6.0 mg) was firstly stirred in 1.0 mL of DMF overnight in the dark. Next, the bottle brush and cyclic brush copolymers (30 mg) in 3 mL of DMSO was added to the curcumin solution and stirred at room temperature for 1 h. After stirring for another 1 h to realize drug encapsulation. The solution was placed in a dialysis bag (MWCO: 3.5 kDa) and dialyzed against 5 L of distilled water 24 h, which was renewed every 3 h at initial 12 h to remove DMF, DMSO and unloaded curcumin. Finally, the BB@Cur and CB@Cur were harvested by lyophilization. To determine the drug loading content (DLC) and entrapment efficiency (EE), the freeze-dried drug-loaded micelles were re-dispersed in phosphate buffer (PBS, pH=7.4, 150 mM). The concentration of Cur was determined by

measuring the absorbance at 436 nm using a Lambda 35 UV-Vis spectrometer (Perkin- Elmer). The DLC and EE were calculated using the following formula,

$$DLC\,(\%) = W_{\text{drug loaded in particles}} / W_{\text{particles}} \times 100\% \qquad (1)$$

$$EE\,(\%) = W_{\text{drug loaded in particles}} / W_{\text{drug fed for encapsulation}} \times 100\% \qquad (2)$$

The hydrophilic drug LXP is encapsulated in the same way. Briefly, the hydrophilic drug LXP (4.0 mg) was stirred in 1.0 mL of H_2O overnight in the dark. Next, the BB, CB, BB@Cur and CB@Cur (20 mg) in 2 mL of DMSO was added to the LXP solution and stirred at room temperature for 1 h. After stirring for another 1 h to realize drug encapsulation. The drug solution was lyophilized after dialysis to obtain BB@LXP, CB@LXP, BB@Cur@LXP and CB@Cur@LXP. The freeze-dried drug-loaded micelles were re-dispersed in PBS, the concentration of LXP was determined by measuring the absorbance at 220 nm using a Lambda 35 UV-Vis spectrometer (Perkin- Elmer). The DLC and EE were calculated using the above same formula.

In vitro drug release studies were conducted in eight groups. Four groups were drug release of CB@Cur, CB@LXP, BB@Cur@LXP and CB@Cur@LXP in pure PBS (pH 7.4, 150 mM), and the other four groups were drug release behavior of CB@Cur, CB@LXP, BB@Cur@LXP and CB@Cur@LXP in PBS (pH 5.5, 150 mM). Briefly, the lyophilized CB@Cur, CB@LXP, BB@Cur@LXP and CB@Cur@LXP were re-dispersed in different media to prepare the drug-carrying micelle solution with the concentration of 0.5 mg/mL. 1 mL of the above solution was transferred to a dialysis bag (MWCO= 3.5 kDa), then the bag was immersed into a 100 mL centrifuge tube containing 25 mL of different pH release media, and 4 parallel samples were taken

from each of the two media. The tube was kept in a horizontal laboratory shaker thermostated at a constant temperature of 37 °C and a stirring speed of 120 rpm. In the dark, 3 mL of release medium in tube was taken out at 0.5, 1, 2, 4, 6, 8, 12 h and 1, 2, 3, 4, 5, 6, 7, 8, 9, 10, 11, 12, 13 and 14 day, and replenished with the equivalent volume of fresh medium was supplemented each time. The drug concentration was calculated by measuring the absorbance at 436 and 220 nm according to a standard calibration curve obtained from Cur and LXP in the corresponding release buffers. The experiment was performed in quadruplicate for each sample.

2.0 Cell viability study.

The cytotoxicity of various formulations was evaluated *in vitro* using the CCK-8 assay. The rat chondrocytes cells (Procell Life Science & Technology Co., Ltd., Hubei, China) were cultured to the second generation in a DM/F 12 complete medium containing FBS, growth additives, Penicillin, Streptomycin, etc. Then, the rat chondrocytes were plated in 96-well plates at a density of 3,000 cells per well in 0.1 mL of complete growth medium and incubated in an incubator maintained at 37 °C and 5% CO_2 environment for 24 h. Cur, LXP, BB, CB, BB@Cur@LXP and CB@Cur@LXP were prepared in serial dilutions in sterilized DM/F 12 medium. The cells were then rinsed once with PBS and incubated with 0.1 mL of the sample solutions with different polymer concentrations for 1, 3 and 5 day at 37 °C, respectively. The CCK-8 assay kit was used to measure the cytotoxicity of different formulations. Briefly, the solution (CCK-8/complete DM/F 12 medium=1:10) was added to each well (100 μL), and then incubated at 37 °C for 3 h. The optical density

(OD) value was measured at 450 nm by a microplate reader (ST-360, KHB, China). The cell viability (CV) was calculated according to the following:

$$\text{Cell viability}\,(\%) = \frac{OD_{450} - OD_{blank}}{OD_{control} - OD_{blank}} \times 100\% \qquad (3)$$

2.1 Live/dead staining.

The rat chondrocytes cells were cultured in 96-well plates with the density of 3,000 cells per well in 0.1 mL of complete growth medium and incubated in an incubator maintained at 37 °C and 5% CO_2 environment for 1 day. Cur, LXP, BB, CB, BB@Cur@LXP and CB@Cur@LXP were prepared in serial dilutions in sterilized DMEM medium. The cells were then rinsed once with PBS and incubated with 100 μL of the polymer solutions with different polymer concentrations at 37 °C for 24 h. At 24 h, cells were rinsed three times with PBS, FDA (live cell, green) and PI (dead cell, red) mixture in PBS were utilized to stain chondrocytes cells in the dark for 15 min. The cells were washed with PBS five times and photographed with a 10x fluorescence microscope.

2.2 Morphological staining.

Morphological staining of rat chondrocytes was studied through our previous reports. Briefly, rat chondrocytes cells were seeded in 48-well plates at a plating density of 6,000 cells per well in 250 μL of complete growth medium and incubated in a 37 °C, 5% CO_2 environment for 24 h. Solutions of Cur, LXP, BB, CB, BB@Cur@LXP and CB@Cur@LXP were prepared in complete growth medium and then added to the wells and incubated for 24 h at 37 °C. Cells were later rinsed with PBS and fixed with 4% paraformaldehyde (PFA) solution for 15 min at room temperature. Subsequently,

the cells were permeated with 0.5% Triton X-100 at room temperature for 10 min and washed with PBS five times. Then, the cells were stained with rhodamine-labeled Phalloidin for 30 min. After that, the cells were washed with PBS five times. Finally, cells were counterstained with 2-(4-amidinophenyl)-6-indolecarbamidine (DAPI) for 10 min, rinsed thoroughly with PBS for 5 times, and observed by fluorescence microscope.

2.3 qRT-PCR.

To evaluate whether CB affect the expression of inflammatory factors associated with OA, we detected the expression of inflammatory factors in chondrocytes co-cultured with BB, CB, BB@Cur@LXP and CB@Cur@LXP by qRT-PCR. The rat chondrocytes cells were cultured in 6-well plates with the density of 5×10^4 cells per well in 1 mL of complete growth medium, stimulated with 1 μg/mL of Lipopolysaccharide (LPS) for 24 h. Then, chondrocytes and BB, CB, BB@Cur@LXP and CB@Cur@LXP co-cultured for 24 h. TRIzol reagent was used to extract total RNA from the cells after trypsin digestion. The expression levels of Interleukin-1β (IL-1β), Collagen II (Col2α), Aggrecan (AGG), Matrix metalloproteinase-13 (MMP13), neuropeptide (TAC1) and metalloproteinase-5A (Adamts5) were detected by target gene specific primers. The sequences of related primers detected by qRT-PCR were as follows:

Table S1. The related primer sequences.

RNA template	Forward primer (5-3)	Reverse primer (5-3)
β-actin	5’-CACTATCGGCAATGCGGTTCC-3’	5’-CAGCACTGTGTTGGCATAGAGGTC-3’
IL-1β	CAACTGTTCCTGAACTCAACTG	GAAGGAAAAGAAGGTGCTCATG
Col2α	TGGACGATCAGGCGAAACC	GCTGCGGATGCTCTCAATCT
AGG	GTGCCTATCAGGACAAGGTCT	GATGCCTTTCACCACGACTTC
MMP13	CACTCCCTTGGACTCACTCA	CCCATATAAAGCCTGGATGC
TAC1	TTGCAGAGGAAATCGGTGCC	GAACTGCTGAGGCTTGGGTC
Adamts5	TCCTCTTGGTGGCTGACTCTTCC	TGGTTCTCGATGCTTGCATGACTG

2.4 Rat osteoarthritis model and surgical process.

All the experimental animal studies have the approval of animal ethical, and welfare authorized by the Animal Ethics Committee of Sichuan University (KS2020028), from Chengdu West China Experimental Animal Center (Chengdu, China). All the animals were randomly divided into six groups, placed in standard cages and given free access to water and food. All the animals underwent a week of domestication before further testing. Osteoarthritis model of SD rats (8 weeks old, 200-250g, n = 25)

was established via DMM surgery (Figure 6a). Briefly, SD rats were anesthetized with pentobarbital sodium and then moved to the operating table, where anesthesia was maintained with 2% isoflurane and 0.8 L/min oxygen, and the skin around the knee joint was routinely disinfected. Under a minimally invasive surgical microscope, the skin, subcutaneous tissue and joint capsule were cut in the patella of the right knee with a microsurgical knife, and internal meniscus tibial ligament resection was performed to induce early osteoarthritis. The subcutaneous tissue and skin were sutured with absorbable surgical sutures, and the mice were put back into the cage until they fully woke up. One week after surgery, rats in each group (n = 5 for each group) were injected with normal saline (NS), BB, CB, BB@Cur@LXP and CB@Cur@LXP in the articular cavity, and then injected once 2 weeks, and euthanized after 8 weeks of treatment.

2.5 Micro CT reconstruction of the joint analysis.

The rats were sacrificed 8 weeks after DMM surgery, and the knee joint samples were harvested. The samples were fixed with 4% paraformaldehyde for 2 days and rinsed with PBS for further analysis. The distal femur was scanned by a high-resolution micro computed tomography (micro-CT) (Bruker, SKYSCAN 1272) for arthrography, and the relative osteophyte volume was evaluated based on the micro-CT scan and reconstruction results.

2.6 Histological staining and immunohistochemistry staining.

After micro-CT, the knee joint samples were decalcified in 10% ethylene diamine tetraacetic acid (EDTA) for 4 weeks. All samples were dehydrated with ethanol and

embedded within paraffin (Lilai Medical Laboratory Center). Paraffin sections (thickness: 5 μm) were prepared and sections were stained with hematoxylin-eosin (H&E), safranin O-fast green, **Masson's** trichrome staining and collagen type II. The stained sections were scored according to the Osteoarthritis Research Society International (OARSI) criteria.

2.7 qRT-PCR analysis of joint tissue.

In order to further evaluate the lesions and repair of SD rat knee joint tissue, we homogenized the joint tissue, and detected the expression of five inflammatory factors: collagen II (Col 2α), cartilage proteoglycan (aggrecan), tachykinin1(TAC1), Adamalysin-like metalloproteinases with thrombospondin (TS) motifs (ADAMTS)-5 and matrix metalloprotein 13 (MMP13) after centrifugation for 20 minutes.

The sequences of related primers detected by qRT-PCR were as follows:

Table S2. The related primer sequences.

RNA template	Forward primer (5-3)	Reverse primer (5-3)
β-actin	5'-CACTATCGGCAATGCGGTTCC-3'	5'-CAGCACTGTGTTGGCATAGAGGTC-3'
AGG	GTGCCTATCAGGACAAGGTCT	GATGCCTTTCACCACGACTTC
Col2α	TGGACGATCAGGCGAAACC	GCTGCGGATGCTCTCAATCT
MMP13	5'-AACCAAGATGTGGAGTGCCTGATG-3'	5'-CACATCAGACCAGACCTTGAAGGC-3'
TAC1	TTGCAGAGGAAATCGGTGCC	GAACTGCTGAGGCTTGGGTC
Adamts5		TCCTCTTGGTGGCTGACTCTTCC

TGGTTCTCGATGCTTGCATGACTG

2.8 Acute toxicity evaluation in mice.

SD rats were treated with different materials for 8 weeks and fed with standard water and special food. The SD rats were euthanized at a predetermined time, and the blood samples were collected from the eyes for routine blood test (RT) (Lilai Medical Experimental Center), and the serum inflammatory factors (IL-6, TNF-α, PGE2) were detected by centrifugation. Major organs such as heart, liver, spleen, lung and kidney were isolated and histological sections were prepared and stained with hematoxylin and eosin (H&E) for *in vivo* biosafety assessment.

2.9 Detection of serum inflammation in SD rats.

The levels of inflammatory cytokines interleukin-6 (IL-6), tumor necrosis factor (TNF-α) and prostaglandin E2 (PGE2) in serum samples from SD rats were assessed by enzyme-linked immunosorbent assay (ELISA). We took IL-6 as an example: firstly, the blood was naturally coagulated for 10-20 min at room temperature,

centrifuged for 20 min, and the supernatant was collected, and then the procedure was performed according to the kit instructions. Briefly, (1) adding samples of standards: set standard and sample wells, standard wells and sample wells were set, and 50 μL of different concentrations of standard were added to each standard well. (2) Add the sample: add 40 μL of sample dilution and 10 μL of serum supernatant to the sample well in turn (the final dilution of the sample is 5 times). (3) Add the enzyme: in addition to blank wells, add 100 μL enzyme labeling reagent to each well and incubated at 37 °C for 60 min. (4) Washing: after discarding the liquid in the well plate, add diluted washing solution to each well, stand for 30 s, discard, and repeat for 5 times. (5) Chromogenic: add 50 μL of chromogenic reagents A and B to each well in turn, gently shake and mix, and develop color at 37 °C for 15 min in the dark. (6) Determination: add 50 μL of stop solution to each well (the color changed from blue to yellow), and measure the absorbance (OD value) of each well in sequence at a wavelength of 450 nm. Finally, the actual concentration of the sample was calculated according to the standard curve to evaluate the content of IL-6 in the serum. The levels of TNF-α and PGE2 in serum samples were measured by the same method

2.10 Statistical analysis.

All the data were shown as the mean ± SD. All independent measurements were repeated at least three times. $*p < 0.05$, $**p < 0.01$, $***p < 0.001$ and $****p < 0.0001$ calculated by Graphpad Prism 9.0 was regarded as a statistically significant difference.

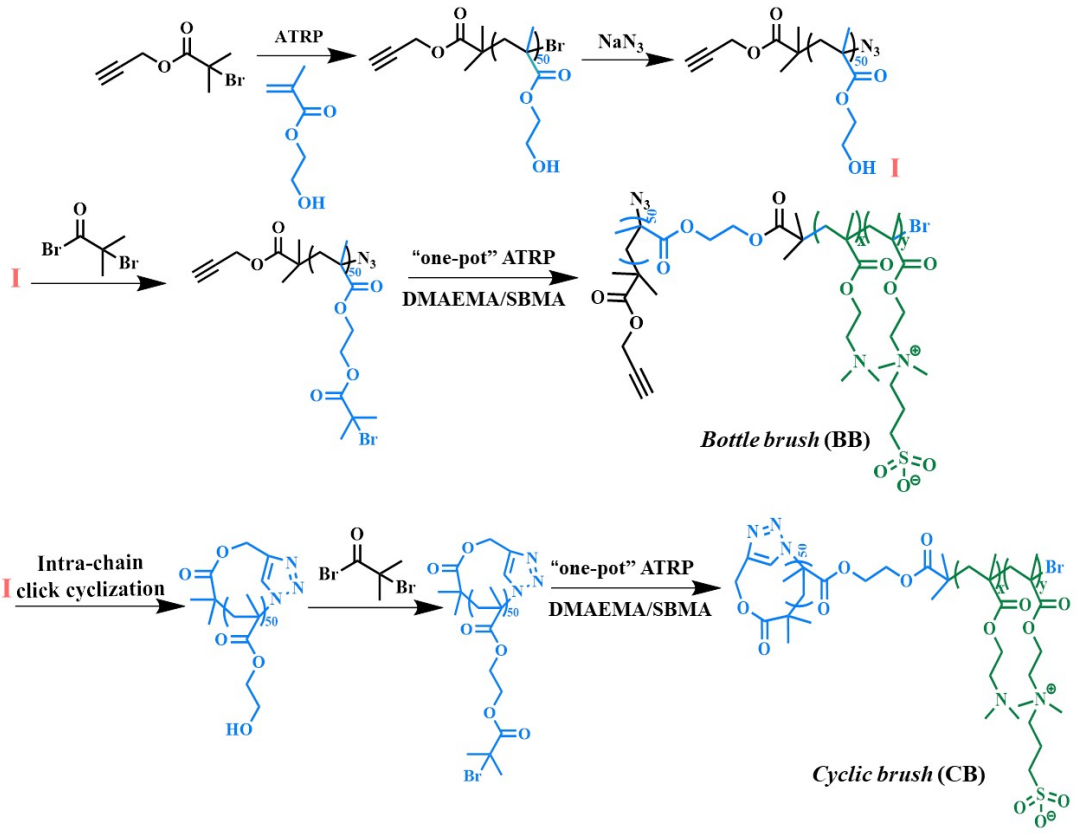

Scheme S1. Synthesis route of Cyclic Brush (CB) and Bottle Brush (BB) polymers.

Table S3. Molecular parameters of the synthesized polymers.

Samples	*M*n [a] (KDa)	*M*n [b] (KDa)	PDI [b]
l-P(HEMA)$_{50}$-Br	6.7	9.5	1.2
l-P(HEMA)$_{50}$-N$_3$	6.6	9.1	1.1
c-P(HEMA)$_{50}$	6.6	8.4	1.1

[a]Determined by ^{1}H NMR, [b]determined by SEC-MALLS.

Table S4. The drug loading (DLC) and encapsulation rate (EE) of bottle brush (BB@Cur) and cyclic brush (CB@Cur).

Sample	DLC (%)	EE (%)
bottle brush (BB)	8.7	43.6
cb-P(HEMA-*g*-P(DMAEMA$_{30}$-*st*-SBMA$_{45}$))$_{50}$ (CB1)	10.5	52.4
cb-P(HEMA-*g*-P(DMAEMA$_{45}$-*st*-SBMA$_{45}$))$_{50}$ (CB2)	10.4	51.9
cb-P(HEMA-*g*-P(DMAEMA$_{60}$-*st*-SBMA$_{45}$))$_{50}$ (CB3)	18.6	92.9
cb-P(HEMA-*g*-P(DMAEMA$_{80}$-*st*-SBMA$_{45}$))$_{50}$ (CB4)	14.9	74.7

Table S5. The drug loading (DLC) and encapsulation rate (EE) of bottle brush (BB@LXP) and cyclic brush (CB@LXP).

Sample	DLC (%)	EE (%)
bottle brush (BB)	10.5	52.6
cb-P(HEMA-*g*-P($DMAEMA_{30}$-*st*-$SBMA_{45}$))$_{50}$ (CB1)	10.5	52.5
cb-P(HEMA-*g*-P($DMAEMA_{45}$-*st*-$SBMA_{45}$))$_{50}$ (CB2)	13.6	68.0
cb-P(HEMA-*g*-P($DMAEMA_{60}$-*st*-$SBMA_{45}$))$_{50}$ (CB3)	16.5	82.7
cb-P(HEMA-*g*-P($DMAEMA_{80}$-*st*-$SBMA_{45}$))$_{50}$ (CB4)	14.1	70.4

Table S6. The kinetics of *in vitro* Cur release.

Model	BB@Cur@LXP pH 7.4	CB@Cur@LXP pH 7.4	BB@Cur@LXP pH 5.5	CB@Cur@LXP pH 5.5
Zero-order	$Q = 0.07\ t + 14.28$ ($R^2 = 0.73$)	$Q = 0.03\ t + 14.23$ ($R^2 = 0.40$)	$Q = 0.17\ t + 31.01$ ($R^2 = 0.77$)	$Q = 0.22\ t + 29.22$ ($R^2 = 0.68$)
First-order	$Ln\ (1-Q) = 0.11\ t + 29.56$ ($R^2 = 0.81$)	$Ln\ (1-Q) = 0.40\ t + 20.89$ ($R^2 = 0.83$)	$Ln\ (1-Q) = 0.10\ t + 66.97$ ($R^2 = 0.77$)	$Ln\ (1-Q) = 0.04\ t + 79.33$ ($R^2 = 0.96$)
Higuchi	$Q = 1.49\ t^{1/2} + 9.79$ ($R^2 = 0.90$)	$Q = 0.73\ t^{1/2} + 11.65$ ($R^2 = 0.61$)	$Q = 3.48\ t^{1/2} + 20.75$ ($R^2 = 0.92$)	$Q = 4.49\ t^{1/2} + 15.05$ ($R^2 = 0.88$)
Korsmeyer-peppas	$Q = 10.25\ t^{0.21}$ ($R^2 = 0.99$)	$Q = 12.21\ t^{0.11}$ ($R^2 = 0.94$)	$Q = 21.71\ t^{0.22}$ ($R^2 = 0.98$)	$Q = 17.82\ t^{0.28}$ ($R^2 = 0.95$)

t The equation was fitted within 14 day.

Q: Cumulative release.

Table S7. The kinetics of *in vitro* LXP release.

Model	BB@Cur@LXP pH 7.4	CB@Cur@LXP pH 7.4	BB@Cur@LXP pH 5.5	CB@Cur@LXP pH 5.5
Zero-order	$Q = 0.08\ t + 19.36$ ($R^2 = 0.67$)	$Q = 0.05\ t + 18.63$ ($R^2 = 0.54$)	$Q = 0.16\ t + 38.86$ ($R^2 = 0.71$)	$Q = 0.19\ t + 46.62$ ($R^2 = 0.64$)
First-order	$Ln\ (1-Q) = 0.16\ t + 35.17$ ($R^2 = 0.78$)	$Ln\ (1-Q) = 0.59\ t + 27.4$ ($R^2 = 0.75$)	$Ln\ (1-Q) = 0.17\ t + 70.57$ ($R^2 = 0.74$)	$Ln\ (1-Q) = 0.13\ t + 86.74$ ($R^2 = 0.78$)
Higuchi	$Q = 1.58\ t^{1/2} + 14.44$	$Q = 1.01\ t^{1/2} + 15.37$	$Q = 3.21\ t^{1/2} + 29.17$	$Q = 3.95\ t^{1/2} + 34.06$

	(R^2 = 0.85)	(R^2 = 0.71)	(R^2 = 0.86)	(R^2 = 0.84)
Korsmeyer-peppas	$Q = 15.10\ t^{0.17}$ (R^2 = 0.99)	$Q = 16.41\ t^{0.11}$ (R^2 = 0.99)	$Q = 30.61\ t^{0.17}$ (R^2 = 0.99)	$Q = 35.48\ t^{0.18}$ (R^2 = 0.98)

t The equation was fitted within 14 day.

Q: Cumulative release.

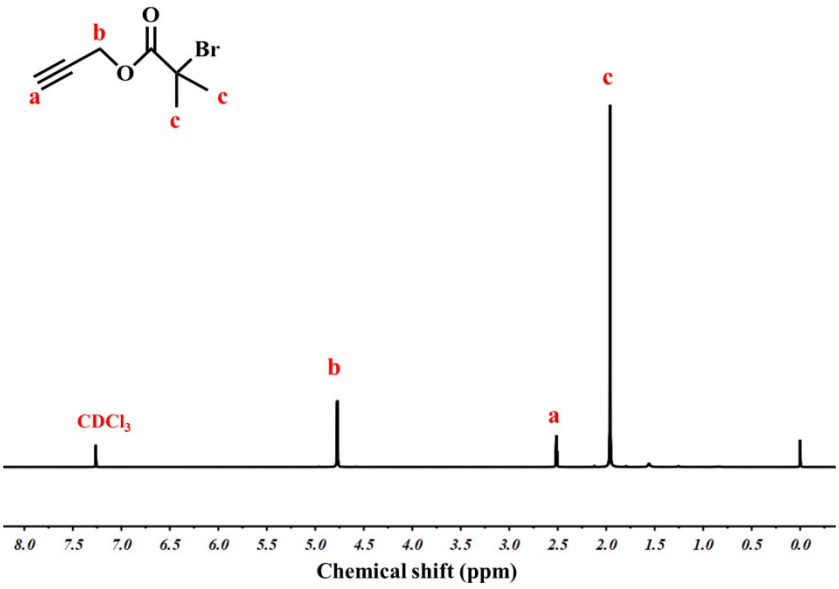

Fig. S1 ^{1}H NMR spectrum of alkyne-Br in $CDCl_3$.

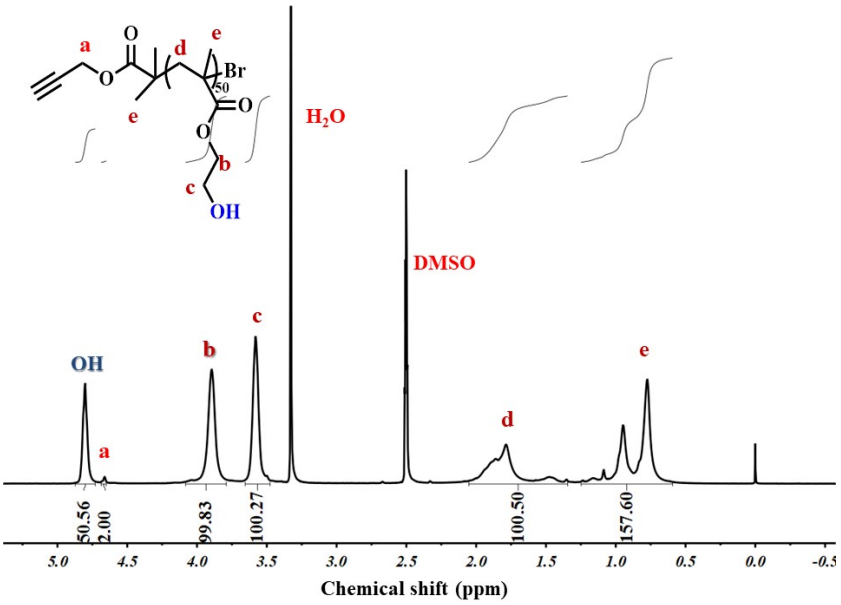

Fig. S2 ^{1}H NMR spectrum of *l*-P(HEMA)$_{50}$-Br in DMSO-*d*6.

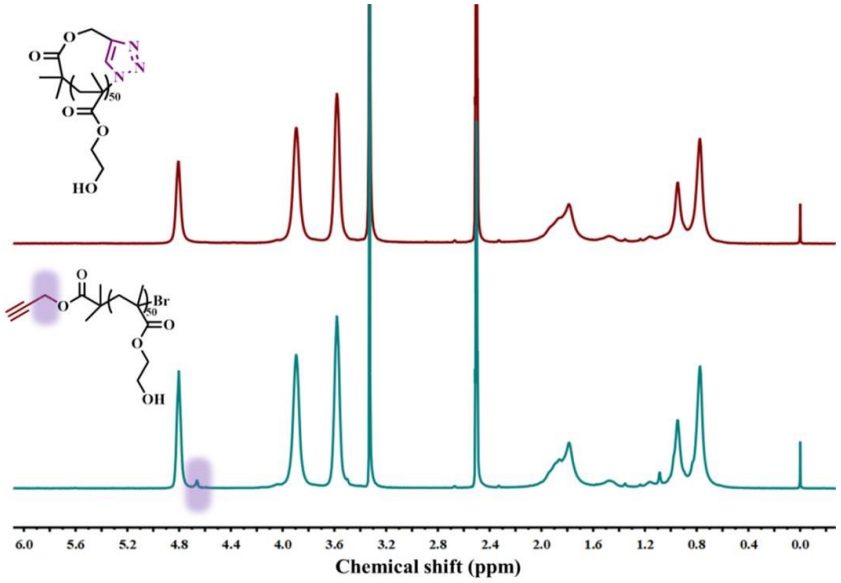

Fig. S3 ^{1}H NMR spectrum of *l*-P(HEMA)$_{50}$-Br and *c*-P(HEMA)$_{50}$ in DMSO-*d*6.

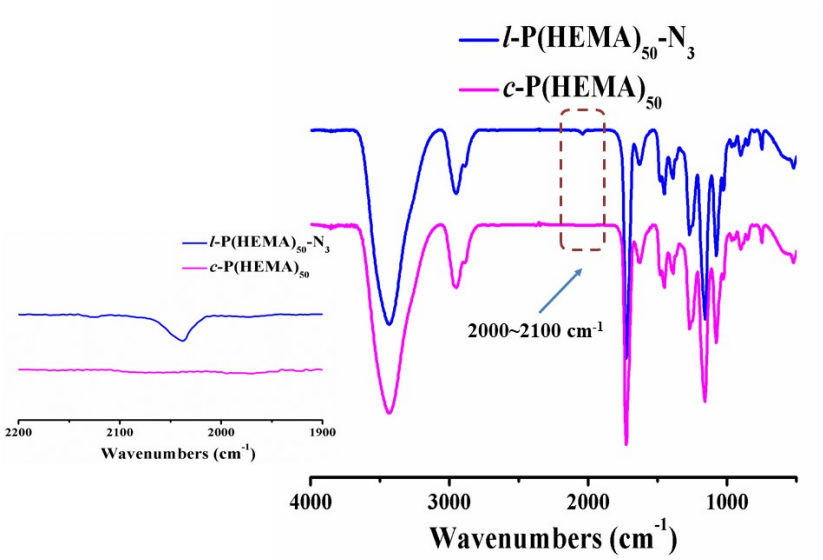

Fig. S4 FT-IR spectrum of *l*-P(HEMA)$_{50}$-N$_3$ and *c*-P(HEMA)$_{50}$.

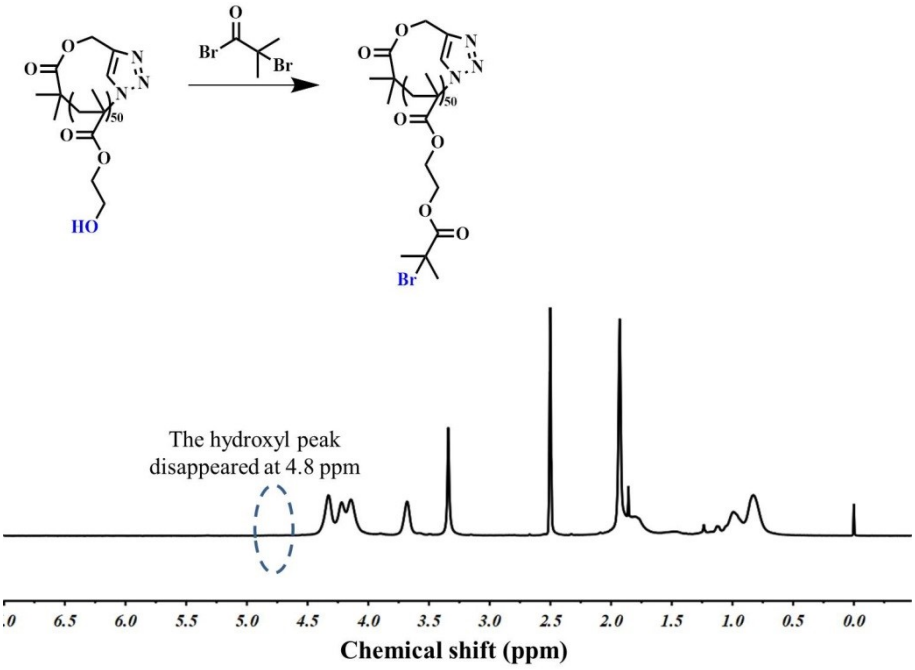

Fig. S5 ^{1}H NMR spectrum of *c*-P(HEMA-Br)$_{50}$ in DMSO-*d*6.

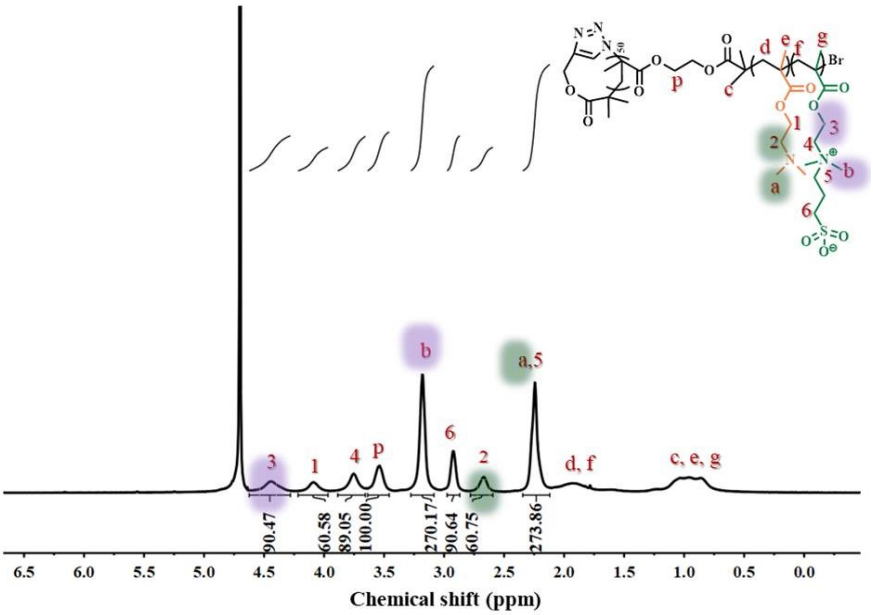

Fig. S6 ^{1}H NMR spectrum of CB1 in D_2O.

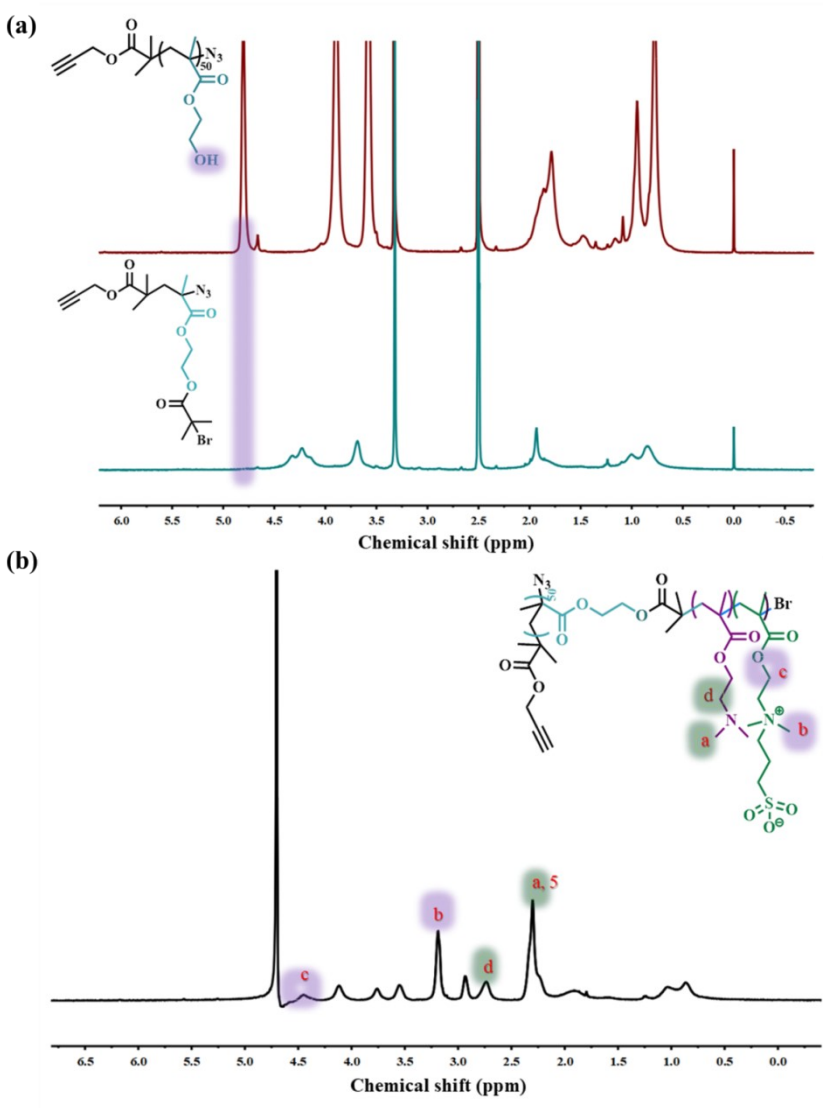

Fig. S7 ^{1}H NMR spectrum of (a) *l*-P(HEMA)$_{50}$-N$_3$ and *l*-P(HEMA-N$_3$)$_{50}$-Br in DMSO-d6 and (b) BB in D_2O.

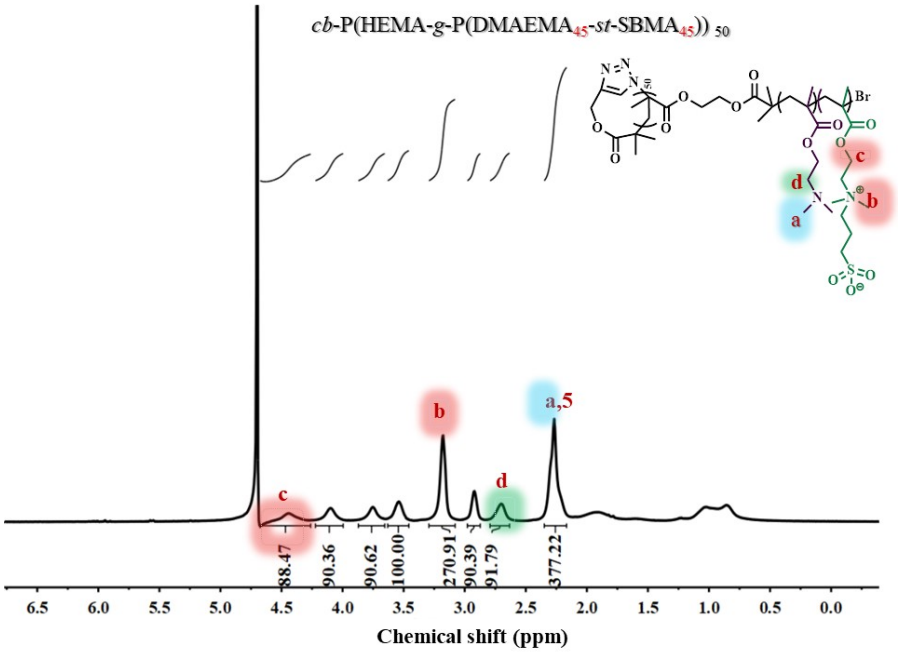

Fig. S8 ^{1}H NMR spectrum of CB2 in D_2O.

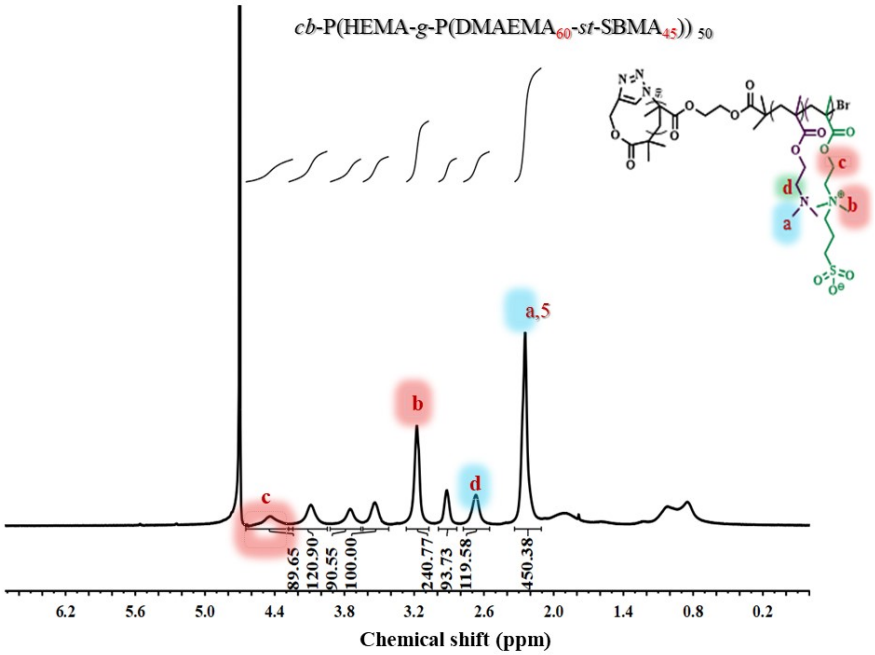

Fig. S9 ^{1}H NMR spectrum of CB3 in D_2O.

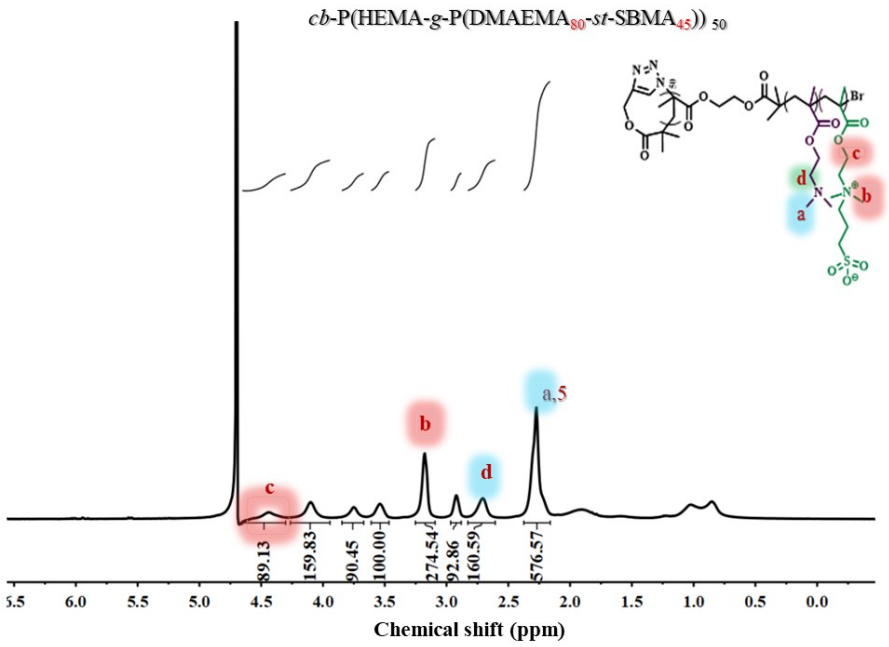

Fig. S10 ^{1}H NMR spectrum of CB4 in D_2O.

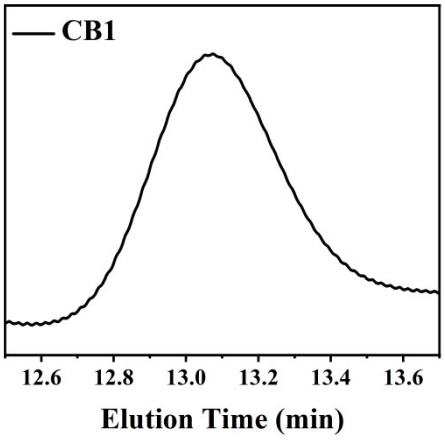

Fig. S11 SEC elution traces of CB1 using H_2O as an eluent.

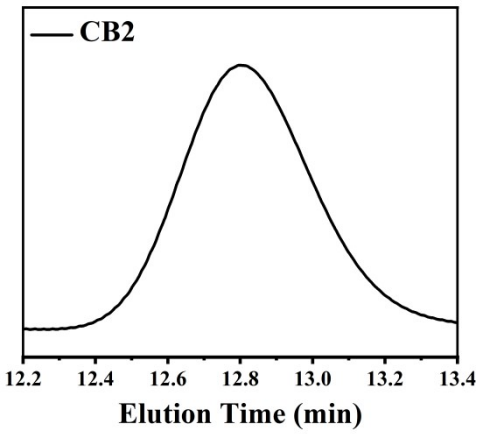

Fig. S12 SEC elution traces of CB2 using H_2O as an eluent.

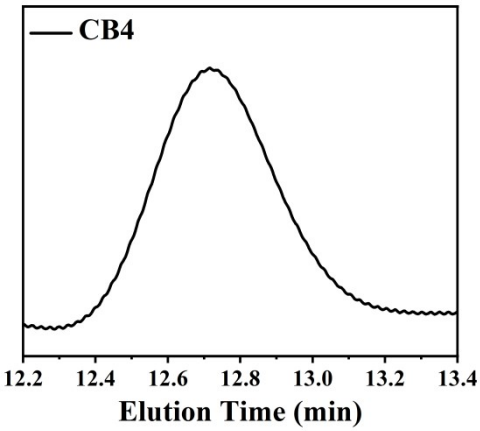

Fig. S13 SEC elution traces of CB4 using H_2O as an eluent.

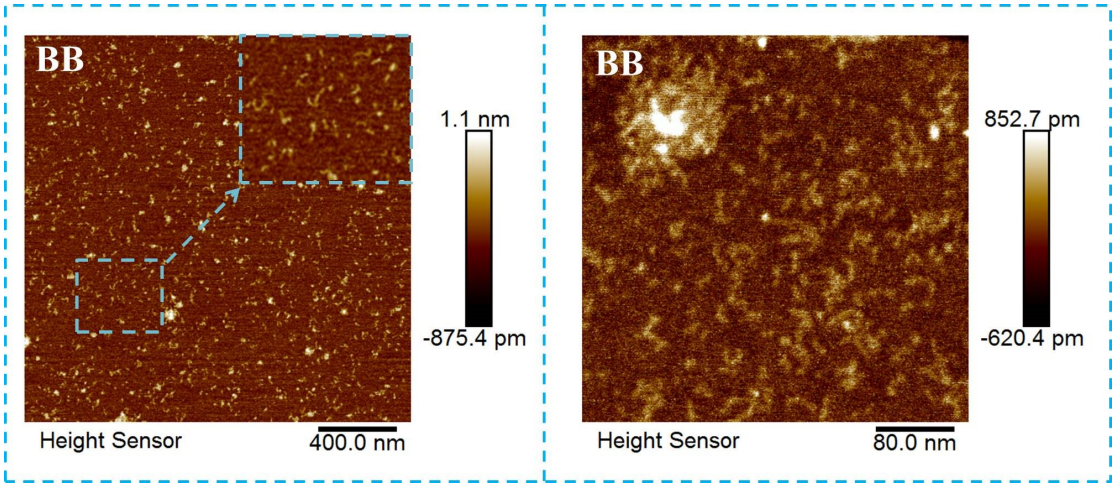

Fig. S14 AFM height images of BB.

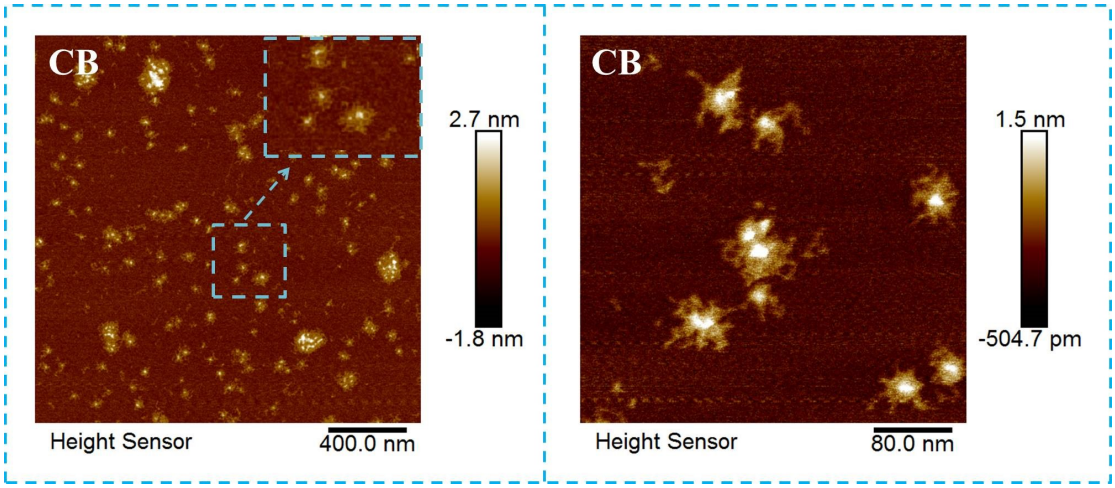

Fig. S15 AFM height images of CB.

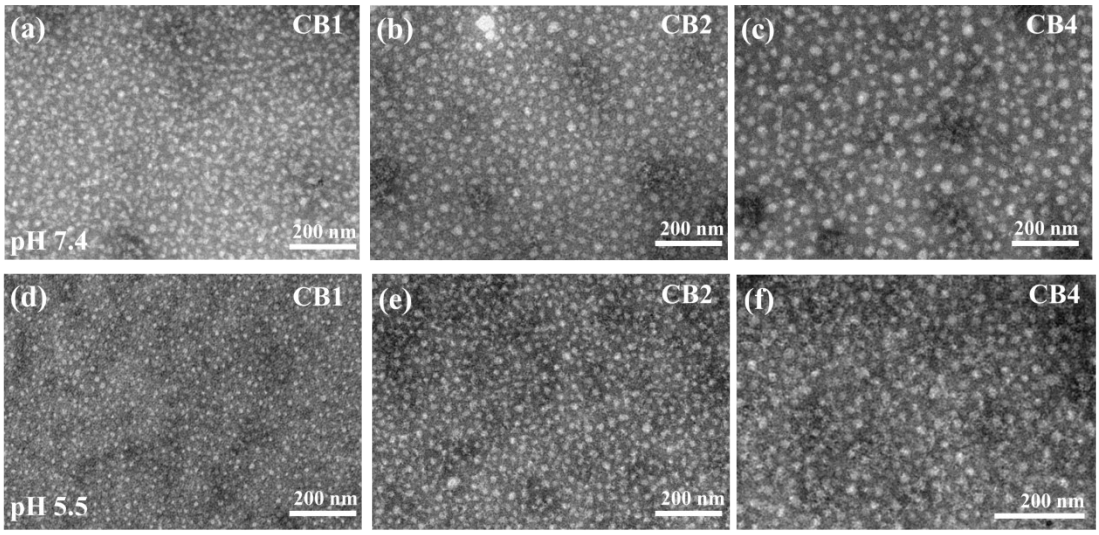

Fig. S16 TEM images of CB1, CB2 and CB4 at pH 7.4 (a-c) and pH 5.5 (d-f).

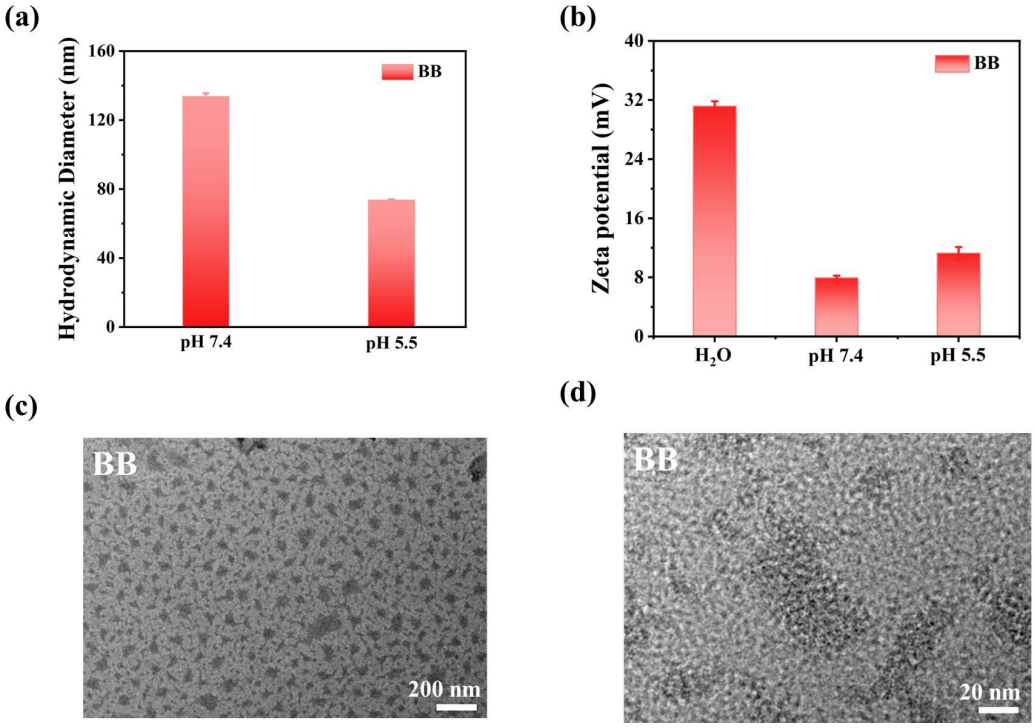

Fig. S17 (a) Hydrodynamic diameters of BB at pH 7.4 and pH 5.5 measured by DLS, (b) Zeta potentials of BB in water and PBS with different pH values and (c, d) TEM images of BB.

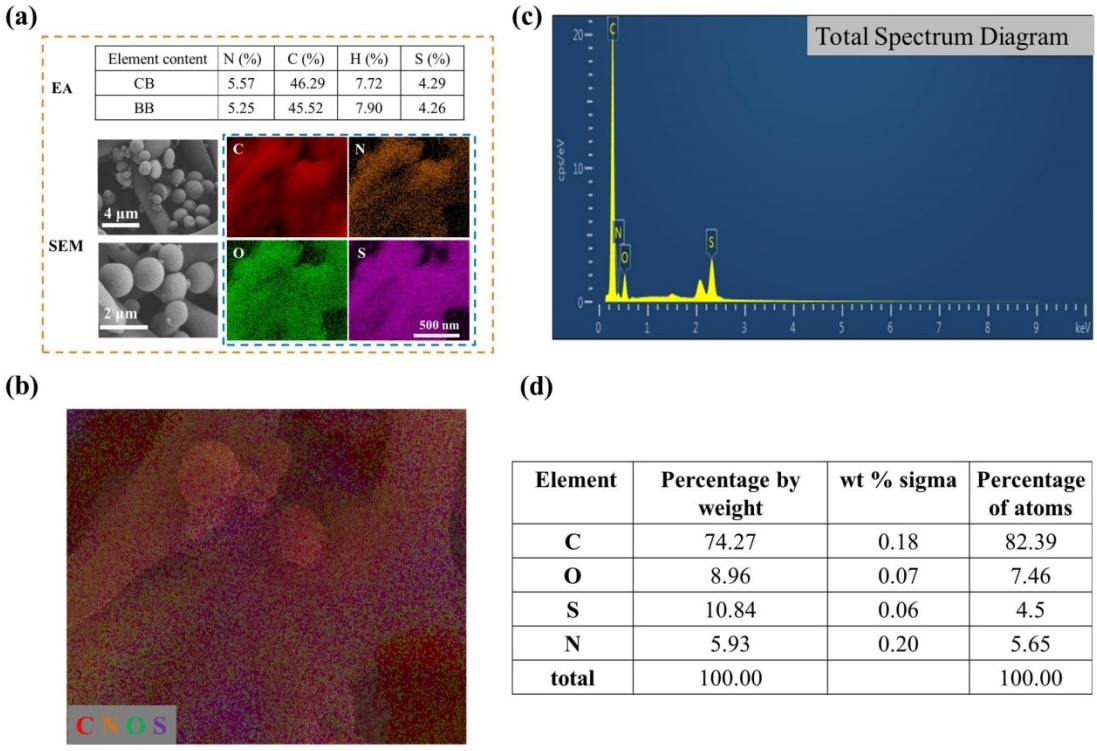

Element	Percentage by weight	wt % sigma	Percentage of atoms
C	74.27	0.18	82.39
O	8.96	0.07	7.46
S	10.84	0.06	4.5
N	5.93	0.20	5.65
total	100.00		100.00

Fig. S18 (a-d) Analysis of N, C, H and S elements of BB and CB polymers and SEM image of CB and corresponding EDX elemental mapping images of C, N, O and S, respectively.

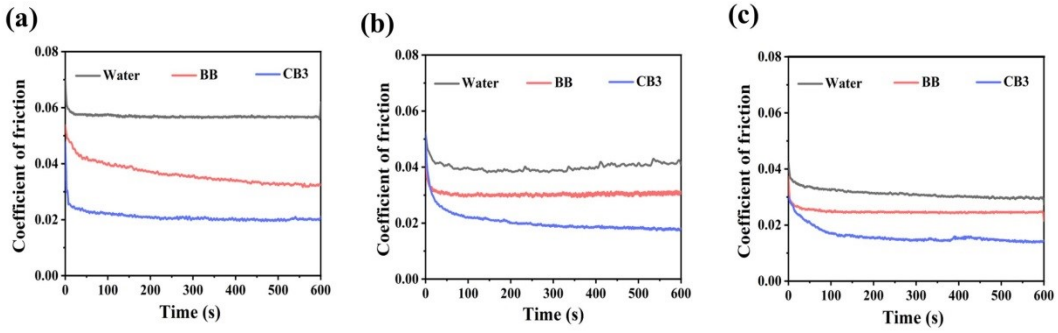

Fig. S19 COF–time curve for water, BB and CB (0.25 mg/mL) at (a) 1 Hz, 1 N; (b) 1 Hz, 3 N and (c) 3 Hz, 3 N.

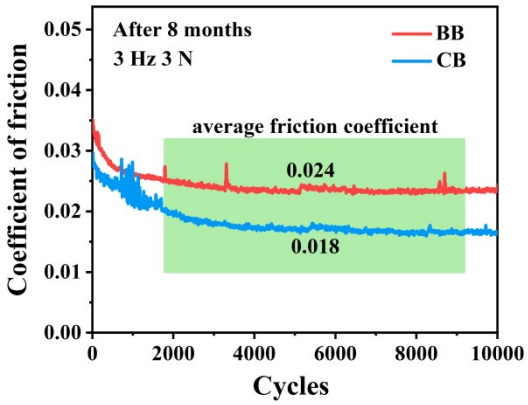

Fig. S20 The friction coefficient of BB and CB (stored for 8 months) during the 10000 friction cycles (3 Hz, 3 N)

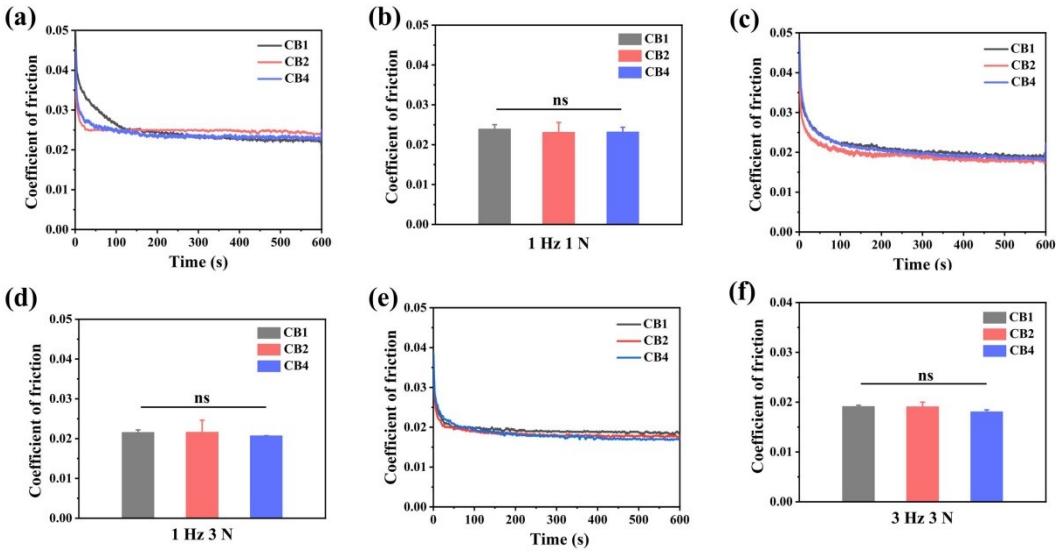

Fig. S21 COF time curves and histograms of CB1, CB2 and CB4 at (a, b) 1 Hz, 1 N, (c, d) 1 Hz, 3 N and (e, f) 3 Hz, 3 N, respectively.

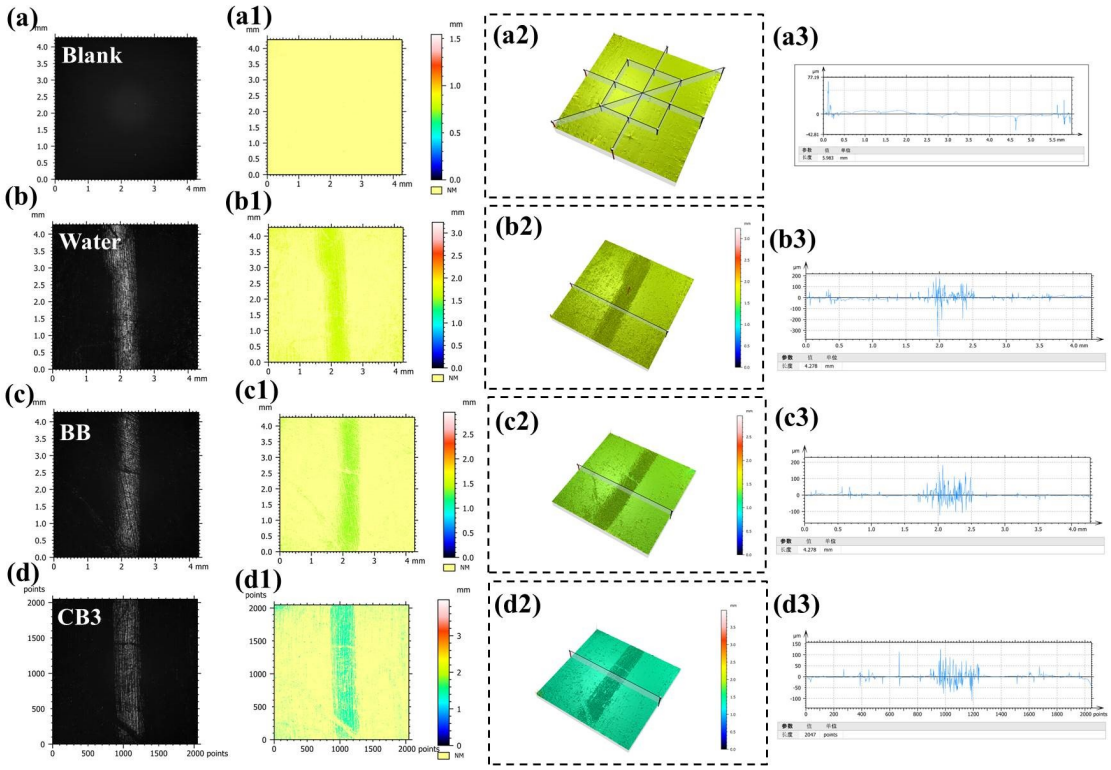

Fig. S22 Surface wear morphology of (a) blank, (b) water, (c) BB and (d) CB.

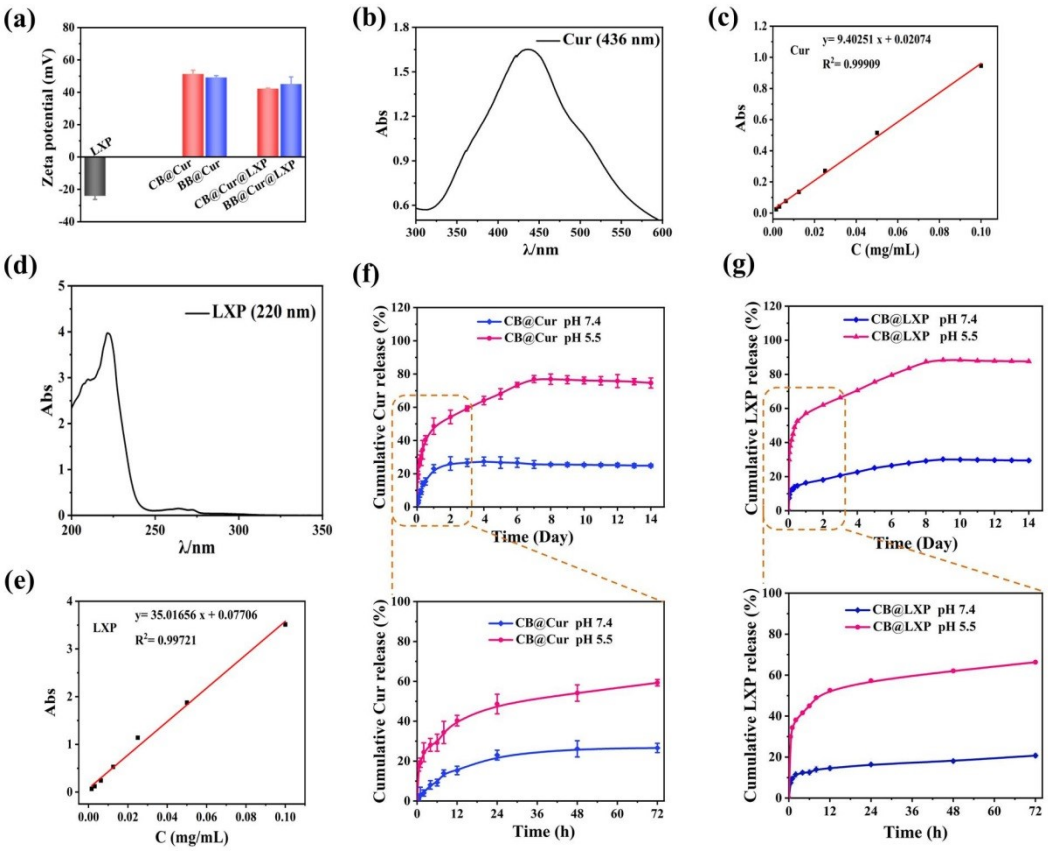

Fig. S23 (a) The zeta potential of LXP, BB@Cur, CB@Cur, BB@Cur@LXP and CB@Cur@LXP, (b, d) the UV–Vis absorbance spectra of (b) Cur and (d) LXP solution, (c, e) the standard calibration curve of (c) Cur and (e) LXP, The drug releasing curves of (f) Cur and (g) LXP from CB@Cur and CB@LXP.

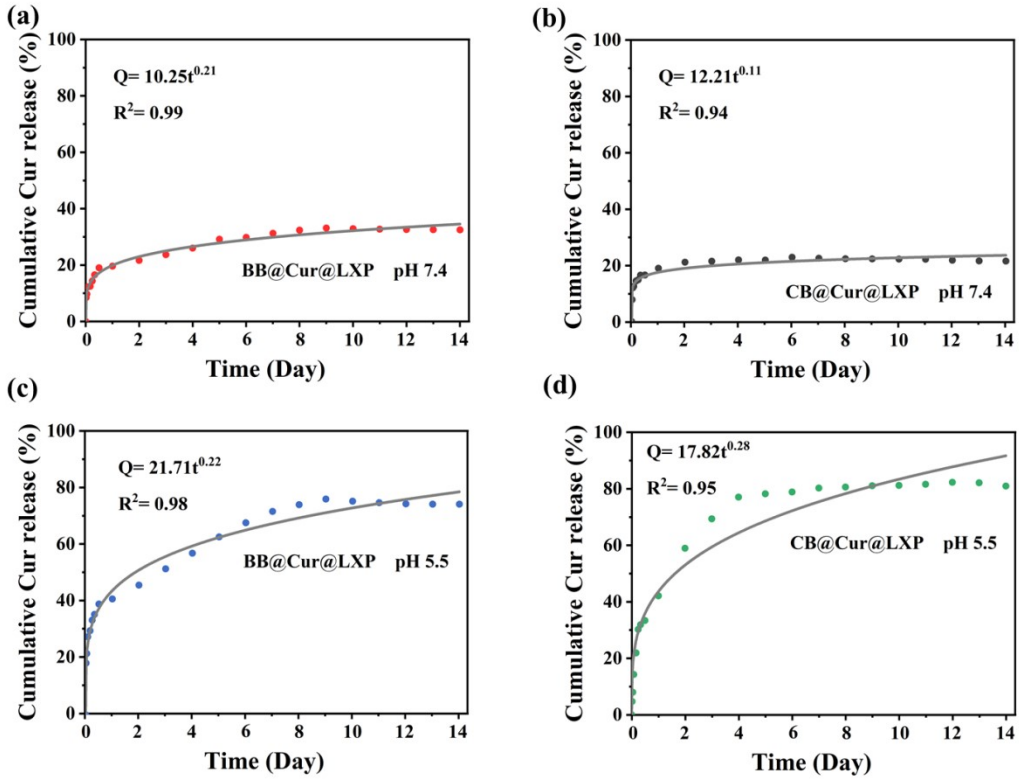

Fig. S24 (a-d) Mathematical analysis of Cur release models for BB@Cur@LXP and CB@Cur@LXP at pH 7.4 and pH 5.5.

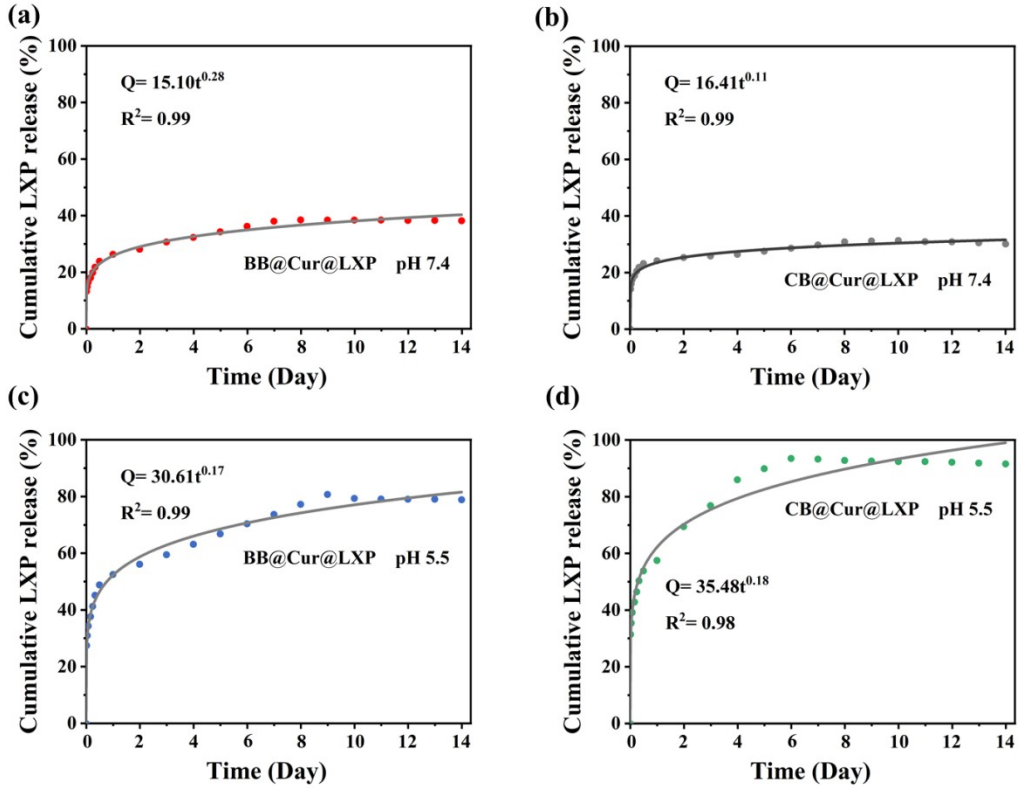

Fig. S25 (a-d) Mathematical analysis of LXP release models for BB@Cur@LXP and CB@Cur@LXP at pH 7.4 and pH 5.5.

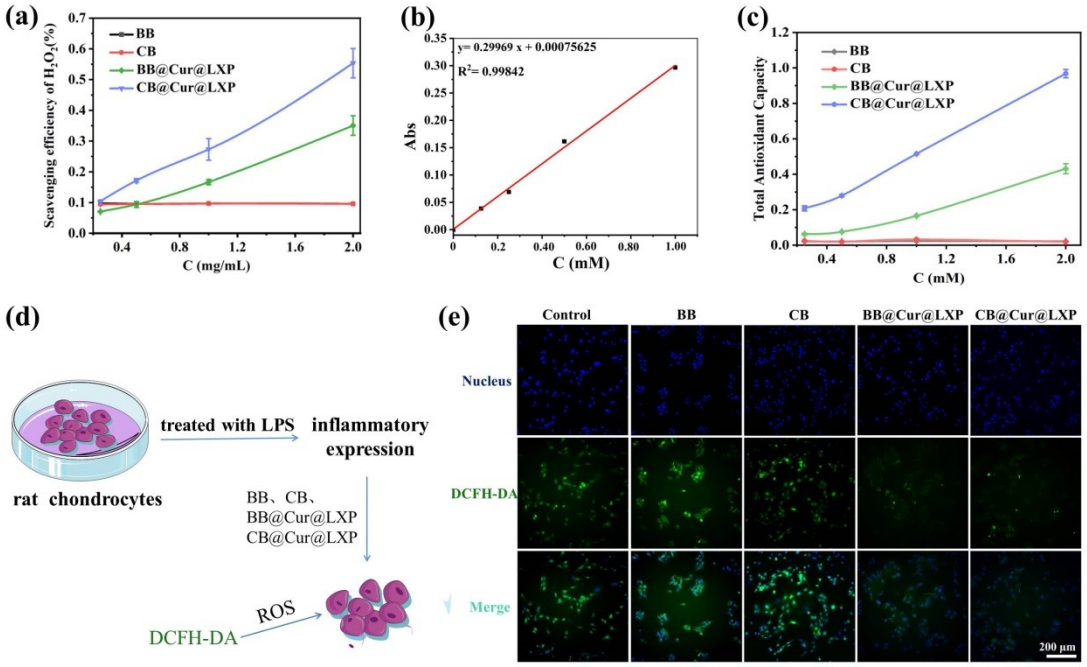

Fig. S26 (a) H_2O_2 scavenging efficiency of BB, CB, BB@Cur@LXP and CB@Cur@LXP, (b) standard curve of total antioxidant capacity, (c) total antioxidant capacity of BB, CB, BB@Cur@LXP and CB@Cur@LXP and (d, e) ROS fluorescence images of chondrocyte after incubation with different materials using DCFH-DA.

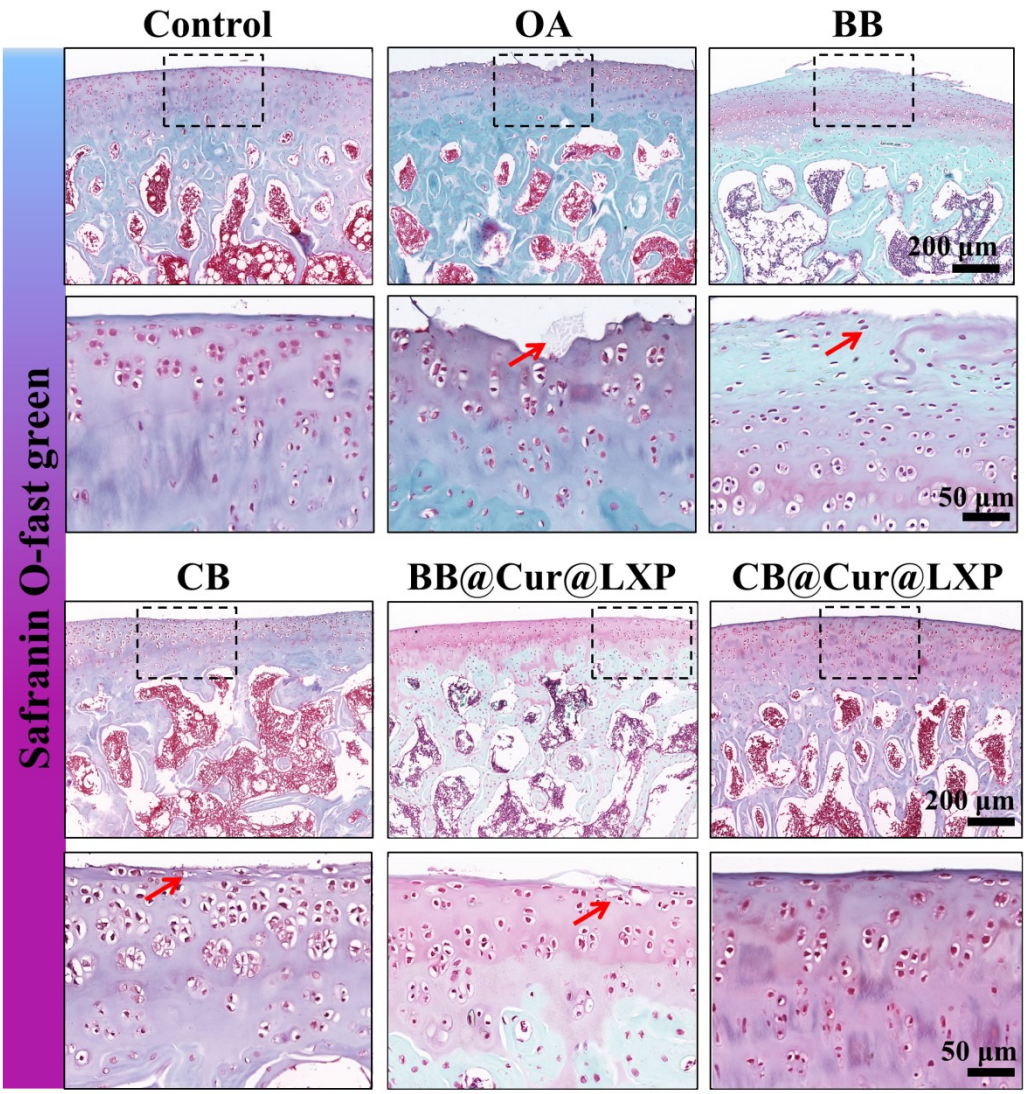

Fig. S27 Representative Safranin O-fast green staining of the cartilage sections, red arrow represents erosion defect of articular cartilage.

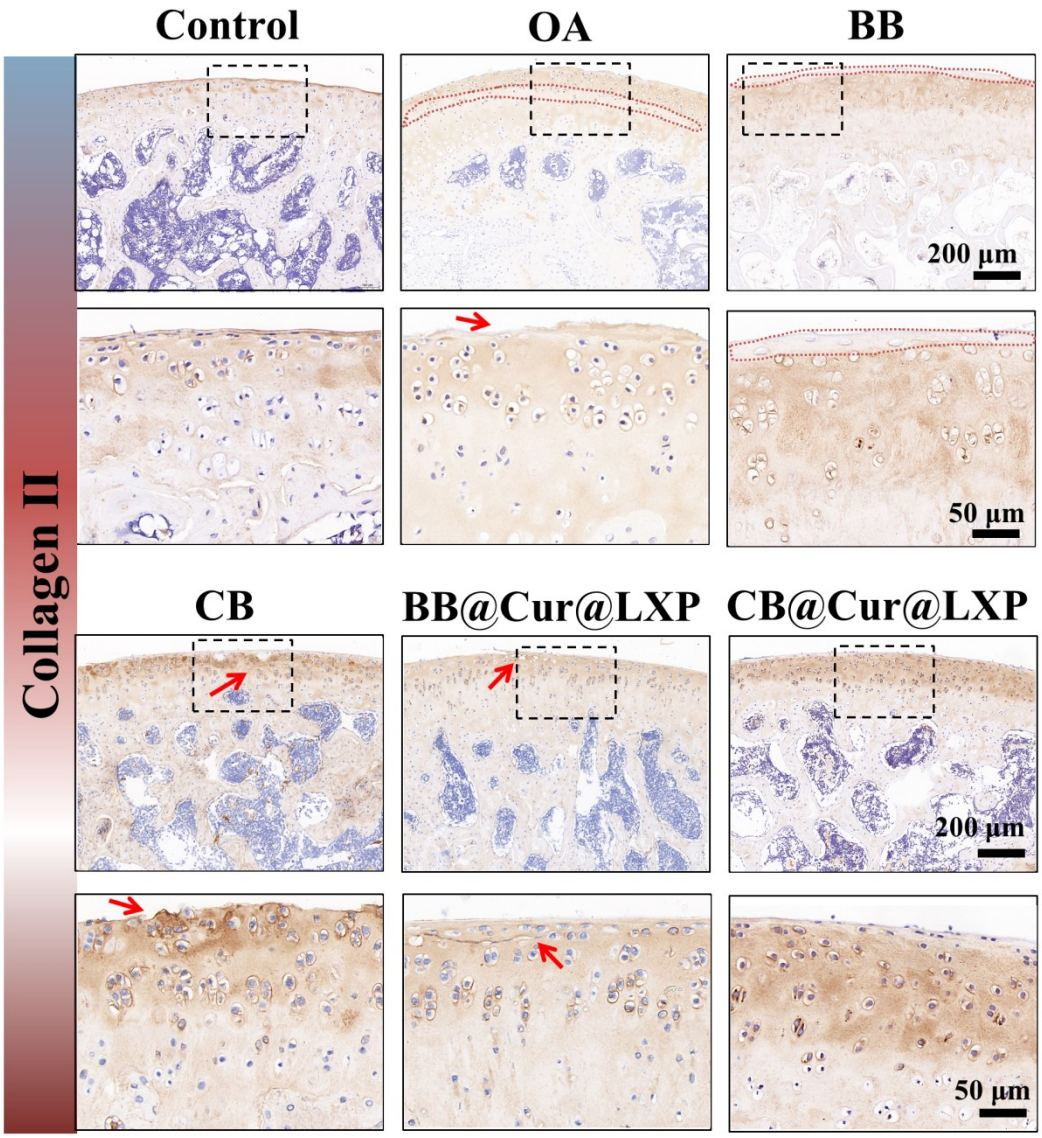

Fig. S28 Representative sections of immunohistochemical staining for collagen II. Red arrow represents erosion defect of articular cartilage, and brown circle indicates loss of collagen II.

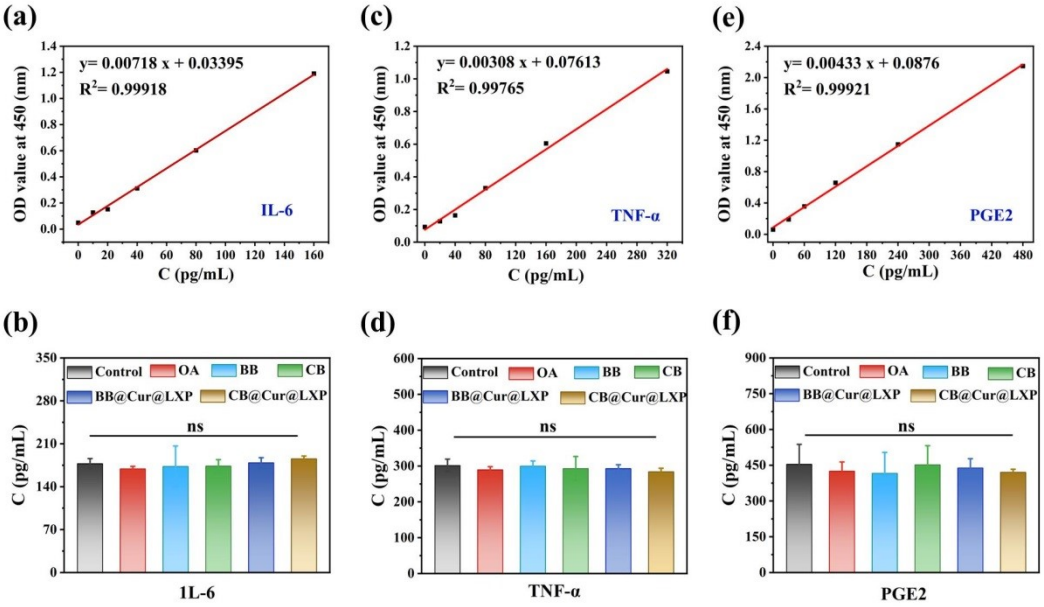

Fig. S29 Detection of serum inflammatory factors in SD rats. (a, c and e) standard curve and expression (b, d and f) of serum inflammatory cytokines IL-6, TNF-α and PGE2 in SD rats with different therapeutic agents.

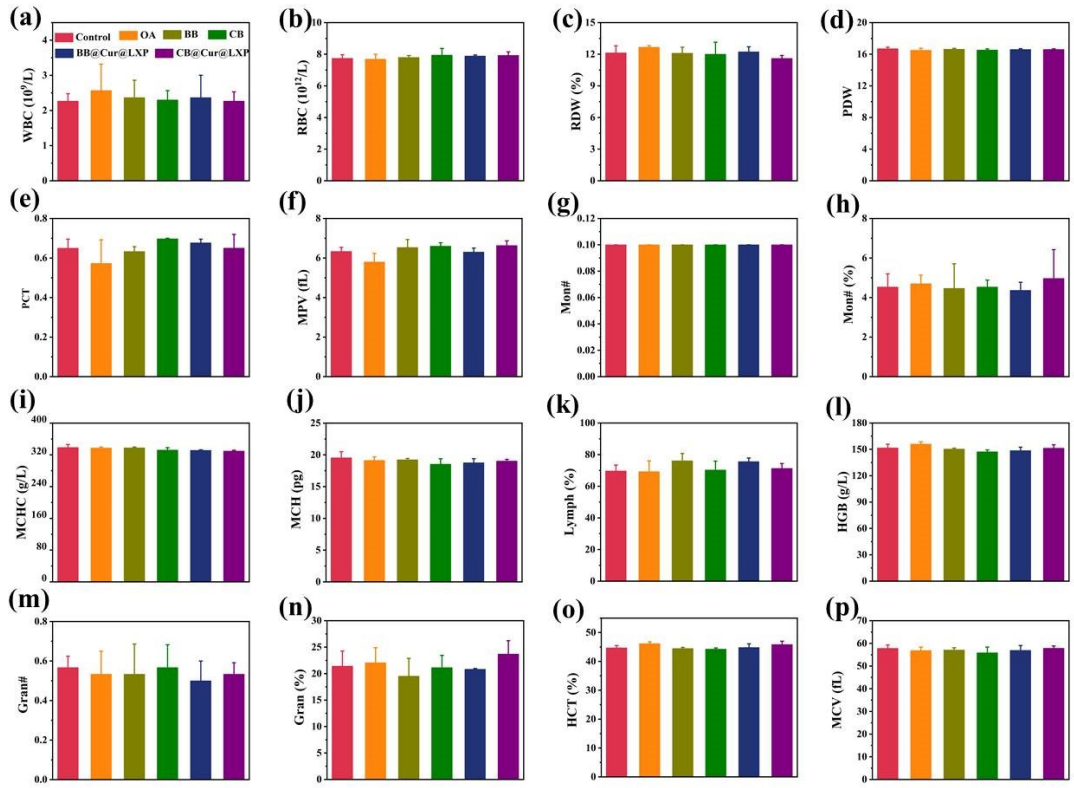

Fig. S30 Hematology and blood biochemistry analysis of the rats injected with different therapeutic agents for 8 weeks. (a) White blood cells (WBC), (b) red blood cells (RBC), (c) red blood cell distribution width (RDW), (d) platelet distribution width (PDW), (e) platelet volume (PCT), (f) mean platelet volume (MPV), (g) number of monocytes (Mon$^{\#}$), (h) percentage of monocytes (Mon%), (i) mean corpuscular hemoglobin concentration (MCHC), (j) mean corpuscular hemoglobin (MCH), (k) percentage of lymphocytes (Lymph%), (l) hemoglobin (HGB), (m) number of neutrophils (Gran$^{\#}$), (n) percentage of neutrophils (Gran%), (o) hematocrit volume (HCT), (p) mean corpuscular volume (MCV).

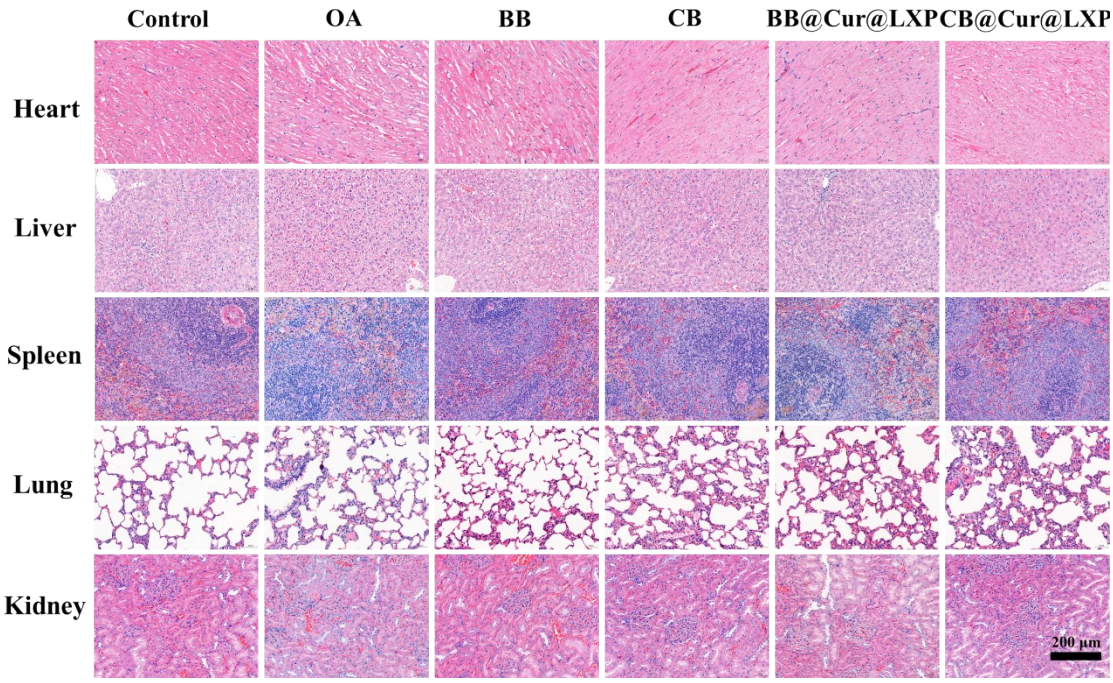

Fig. S31 Histological analyses of the major organs (heart, liver, spleen, lungs, and kidneys) after injection of different preparations for 8 weeks.

Reference

[1] X. H. He, C. Y. Gao, W. Q. Sun, W. Huang, S. L. Lin and D. Y. Yan, *Polym. Chem*., 2013, **51**, 1040–1050.

[2] X. Y. Tu, C. Meng, X. L. Zhang, M. G. Jin, X. S. Zhang, X. Z. Zhao, Y. F. Wang, L. W. Ma, B. Y. Wang, M. Z. Liu and H. Wei, *Macromol. Biosci*., 2018, **18**, 1800022.

[3] M. Zhang, S. Li, J. L. Peng, Y. Liu, F. J. Liu, F. M. Zhong, S. S. Tang , Q. Ning, C-Y. Yu and H. Wei, *Mater. Today Chem*., 2022, **26**, 100996.

[4] Y. Chen, G. Li, Y. Y. Qian, M. Cai, H. Yin, L. Xiao, W. Tang, F. J. Guo and B. Y. Shi, *Oxid Med Cell Longev*., 2016, **2016**, 3406802.

[5] D. Y. Zhang, Y. Wan, J. Y. Xu, G. H. Wu, L. Li and X. H. Yao, *Carbohydr Polym*., 2016, **137**, 473-479.